Compatibility stresses in deformed bicrystals

J. Gemperlová, V. Paidar, F. Kroupa

COMPATIBILITY STRESSES IN DEFORMED BICRYSTALS

J. Gemperlová, V. Paidar

Institute of Physics, Czechosl. Acad. Sci., Na Slovance 2, 180 40 Praha 8, Czechoslovakia

F. Kroupa

Institute of Plasma Physics, Czechosl. Acad. Sci., Pod vodárenskou věží 4, 182 11 Praha 8, Czechoslovakia

Compatibility stresses have been calculated in the model of a bicrystal composed of two semi-infinite crystals. The elastic anisotropy of the component crystals is fully taken into account. Various particular cases chosen for the cubic bicrystals with the ⟨100⟩ and ⟨110⟩ rotation axes commonly used in experiments are discussed in detail. The effects of elastic and plastic deformation have also been compared. The model provides compatibility stresses as functions of grain boundary geometrical parameters and of the loading axis orientation.

1. INTRODUCTION

Grain boundaries affect mechanical properties of polycrystalline materials in several ways which can be described on different levels starting from the macroscopic level of continuum mechanics up to the microscopic level of atomistic physics. Due to the crystalline elastic anisotropy and the anisotropy of plastic deformation of individual grains, the requirement of strain compatibilities at the grain boundaries leads to additional stresses which must be considered together with the applied stress. This macroscopic effect of grain boundaries will be discussed in detail for a model bicrystal in the present paper.

Macroscopic compatibility effects have been discussed in a large number of papers (see e.g. [1–7]), usually in connection with the activation of additional slip systems in the vicinity of a grain boundary. The secondary slip was observed even in bicrystals with the identical orientation of the primary slip plane in both component crystals [3, 5]. The secondary slip was localized in a narrow region with the grain boundary in its centre and was observed even in places without any primary slip. The occurrence of the secondary slip was explained by the effect of compatibility stresses. The activated slip system was that one for which the total resolved shear stress (composed of the applied and compatibility stresses) was maximum.

The calculation of compatibility stresses for an infinite bicrystal formed by two crystals filling the half-spaces separated by the planar boundary was carried out in [6–9]. The crystals were considered elastically isotropic and therefore, only the effect of homogeneous plastic deformation different in two grains was analyzed. The incompatibility of plastic deformation at the boundary is accommodated by elastic strains in the case of small differences in plastic strains. The additional stresses were calculated using Kröner's theory of continuous distribution of dislocations. The tensor of surface dislocation density was given by differences of plastic strains.

It was shown that the additional stresses are constant in the two grains and change the sign at the boundary.

In this paper we will introduce a physically simple model for the calculation of additional stresses induced by both crystal elastic anisotropy and plastic anisotropy of deformation. The bicrystal is considered as two half-spaces corresponding to crystals with different crystallographic orientations. Elastic anisotropy due to the crystal symmetry is fully respected. The model allows to analyse the dependence of the additional compatibility stresses on various geometrical parameters which determine the type of grain boundary (the orientation of rotation axis, the misorientation angle and the orientation of boundary normal) and the direction of loading axis of tensile or compressive deformation. As far as we know, only particular cases, i.e. bicrystals with special orientations, have been studied in literature and the problem of additional compatibility stresses has not yet been systematically investigated in the frame of anisotropic theory of elasticity.

2. GENERAL FORMULAS

2.1. Finite bicrystal

Let us consider a bicrystal composed of two elastically anisotropic parts A and B which are welded together on plane $x_2 = 0$ (fig. 1a). The bicrystal is loaded at the surface with local normal $\boldsymbol{v}$ by external stress vector

$$F_j = v_i \Sigma_{ij} ,$$

where $\Sigma_{ij} = \Sigma_{ji}$ are constants. Such loading would lead to constant stresses Σ_{ij} in any elastically homogeneous body, anisotropic or isotropic. These constant stresses Σ_{ij} will be called applied stresses.

However, additional stresses τ_{ij} (the so called compatibility stresses) will appear in a bicrystal with a welded boundary. The total stresses σ_{ij} in the bicrystal can be imagined as a sum of the applied and compatibility stresses

$$\sigma_{ij} = \Sigma_{ij} + \tau_{ij} . \tag{1a}$$

The stresses σ_{ij} must fulfil the boundary conditions on the bicrystal surface

$$v_i \sigma_{ij} = F_j = v_i \Sigma_{ij} \tag{1b}$$

and the conditions at the interface $x_2 = 0$,

$$\sigma_{i2}^{\mathrm{A}} = \sigma_{i2}^{\mathrm{B}} . \tag{1c}$$

At the welded interface, other three conditions hold for the total strains ε_{ij} (which will be in general case a sum of the elastic and plastic strains)

$$\varepsilon_{11}^{\mathrm{A}} = \varepsilon_{11}^{\mathrm{B}} , \quad \varepsilon_{33}^{\mathrm{A}} = \varepsilon_{33}^{\mathrm{B}} , \quad \varepsilon_{13}^{\mathrm{A}} = \varepsilon_{13}^{\mathrm{B}} . \tag{1d}$$

The relations (1a, 1b, 1c, 1d) must be valid in a finite bicrystal under external surface forces F_j. However, the solution of the equations of the anisotropic theory of elasticity for this problem is complicated and can be practically found using numerical methods. The distribution of stresses σ_{ij} (i.e. also of compatibility stresses τ_{ij}) is non-homogeneous and depends on the form of the bicrystal. The compatibility stresses τ_{ij} reach high values in the vicinity of the interface $x_2 = 0$ and might approach infinity at the edge of the interface, i.e. at the line of intersection of the interface with the surface (see discussion in section 4 and papers [6, 7, 9, 10]).

The situation near the interface and far from the external surface can be modelled in a simplified way in an infinite medium.

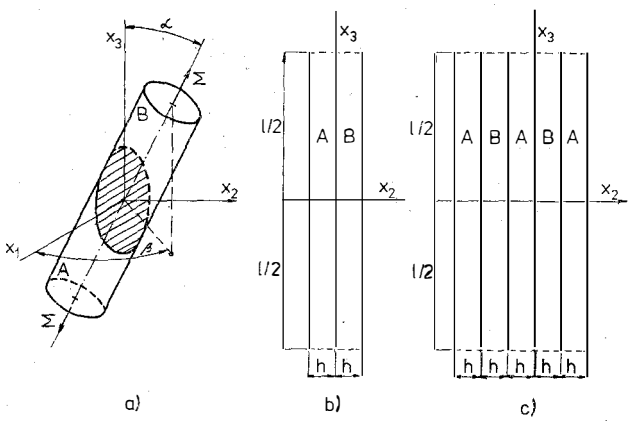

Fig. 1. a) The orientation of the loading axis. The x_2 coordinate axis is perpendicular to the grain boundary plane. The angle between the loading axis and x_3 is denoted as α and between the projection of the loading axis on the x_1x_2 plane and the x_1 direction as β. b) Model of the central part of a finite bicrystal: an infinite bicrystal with $l \to \infty$, $h \to \infty$. c) Layered body with $l \to \infty$, having under the same boundary conditions $F_j = \nu_i \Sigma_{ij}$ the same constant stresses σ_{ij}^{A} and σ_{ij}^{B} as the infinite bicrystal.

2.2. Infinite bicrystal

An infinite bicrystal can be imagined as the limiting case of two welded plates of the same thickness h and with dimensions l in the x_1 and x_3 directions, for $l \to \infty$ (fig. 1b). Besides the elastic deformation, also plastic deformation e_{ij}^{p} will be considered, which will be supposed homogeneous in parts A and B, i.e. e_{ij}^{Ap} and e_{ij}^{Bp} are given constants.

Then the total deformation ε_{ij} can be written as

$$\varepsilon_{ij}^{A} = e_{ij}^{Ae} + e_{ij}^{Ap} + e_{ij}^{A}, \quad \varepsilon_{ij}^{B} = e_{ij}^{Be} + e_{ij}^{Bp} + e_{ij}^{B}, \tag{2}$$

where the elastic deformation corresponding to stresses σ_{ij} is formally divided into two parts $e_{ij}^{e} + e_{ij}$. The first terms due to applied stress Σ_{ij} follow from Hooke's law

$$e_{ij}^{Ae} = S_{ijkl}^{A} \Sigma_{kl}, \quad e_{ij}^{Be} = S_{ijkl}^{B} \Sigma_{kl} \tag{3}$$

and are, therefore, constants; S_{ijkl} are the elastic compliances. The second terms correspond to compatibility stresses τ_{ij},

$$e_{ij}^{A} = S_{ijkl}^{A}\tau_{kl}^{A}, \quad e_{ij}^{B} = S_{ijkl}^{B}\tau_{kl}^{B} \tag{4}$$

and can be called "induced" elastic deformations. They will appear even in the case when no plastic deformation takes place. We can consider an independent homogeneous plastic deformation which may occur on several slip systems (enumerated by k) characterized by the vector of the slip direction, m_i, and the normal to the slip plane, n_i, and the magnitude of the shear deformation, γ,

$$\begin{aligned} e_{ij}^{Ap} &= \tfrac{1}{2}\sum_{k}\left(m_i^{Ak}n_j^{Ak} + m_j^{Ak}n_i^{Ak}\right)\gamma^{Ak}, \\ e_{ij}^{Bp} &= \tfrac{1}{2}\sum_{k}\left(m_i^{Bk}n_j^{Bk} + m_j^{Bk}n_i^{Bk}\right)\gamma^{Bk}. \end{aligned} \tag{5}$$

If the difference between the deformations of the A and B grains is small, the linear theory of elasticity can be used to determine the additional internal stresses τ_{ij}^{A}, τ_{ij}^{B}.

In the bicrystal the interface conditions for total strains ε_{ij} (1d) and total stresses σ_{ij} (1c) must, of course, be fulfilled. The boundary conditions (1b) must be, however, adapted for the case of an infinite body.

The solution for the infinite body can be directly written as the compatibility stresses τ_{ij}^{A} and τ_{ij}^{B} must be constant. This is well accepted for the case of a layered body [11] composed of an odd number or of an infinite number of plates A and B of the same thickness h (fig. 1c). It then follows for the constant stresses σ_{ij}^{A} and σ_{ij}^{B} from the conditions of equilibrium

$$\begin{aligned} &\sigma_{i2}^{A} = \sigma_{i2}^{B} = \Sigma_{i2}, \quad \sigma_{11}^{A} + \sigma_{11}^{B} = 2\Sigma_{11}, \\ &\sigma_{33}^{A} + \sigma_{33}^{B} = 2\Sigma_{33}, \quad \sigma_{13}^{A} + \sigma_{13}^{B} = 2\Sigma_{13}. \end{aligned}$$

Therefore, for constant components of compatibility stresses we have from (1a)

$$\begin{aligned} &\tau_{i2}^{A} = \tau_{i2}^{B} = 0 \\ &\tau_{11}^{A} + \tau_{11}^{B} = 0, \quad \tau_{33}^{A} + \tau_{33}^{B} = 0, \quad \tau_{13}^{A} + \tau_{13}^{B} = 0. \end{aligned} \tag{6}$$

For finite $l \gg h$, these constant stresses give a good approximation of stresses in the middle part of the layered body, i.e. near the x_2 axis, while at the surfaces $x_1 = x_3 = \frac{1}{2}l$ the boundary condition (1b) must be fulfilled and a redistribution of stresses near the surface follows.

Note that in an infinite layered body the exact solution (6) leads to a formal violation of the boundary conditions (1b) at the infinity for $x_1 \to \infty$ and $x_3 \to \infty$. This is, however, an acceptable violation currently used in an infinite layered body where the boundary condition must be fulfilled for total forces (in our case for the average values of σ_{ij}^{A} and σ_{ij}^{B}, i.e. for Σ_{ij}).

The case of bicrystal (fig. 1b) is more complicated as the homogeneous plastic deformation in part A and B may also lead to elastic bending of thin plates. Never-

theless, if we take the infinite body as a limit $l \to \infty$ and also $h \to \infty$, i.e. the bicrystal is composed of two half spaces A and B, there will be again constant compatibility stresses τ_{ij}^{A} and τ_{ij}^{B} which must fulfil conditions (6). The violation of the boundary conditions (1b) is again acceptable within the model of an infinite body and has been used e.g. in [6, 7, 9] for isotropic half spaces.

Let us note that for the uniqueness of the solution, the ratio of the thickness h_A and h_B of plates A and B, respectively, is important. We have assumed $h_A = h_B = h$ and from the conditions of equilibrium the equations (6) follow. If $h_A \neq h_B$, then again $\tau_{i2}^{A} = \tau_{i2}^{B} = 0$, however

$$h_A\tau_{11}^{A} + h_B\tau_{11}^{B} = 0\,, \quad h_A\tau_{33}^{A} + h_B\tau_{33}^{B} = 0\,, \quad h_A\tau_{13}^{A} + h_B\tau_{13}^{B} = 0\,.$$

The stresses τ_{ij} resulting from condition (6) will be taken as an approximation of compatibility stresses in the middle part of the interface in a finite bicrystal (where the assumption $h_A = h_B$ seems reasonable), i.e. near the point $x_1 = x_2 = x_3 = 0$ in fig. 1a.

2.3. Compatibility stresses

The compatibility stresses in an infinite bicrystal with $l \to \infty$ and $h_A = h_B = h \to \infty$ can be easily calculated from equations (1a), (1d), (2), (3), (4), (5), (6). It follows from Hooke's law (4) that for constant τ_{kl}^{A}, τ_{kl}^{B} also the induced elastic strain components e_{ij}^{A}, e_{ij}^{B} are constant. For the differences $\Delta e_{ij} = e_{ij}^{A} - e_{ij}^{B}$ we have from (4) and (2)

$$\Delta e_{ij} = \varepsilon_{ij}^{A} - \varepsilon_{ij}^{B} + e_{ij}^{Be} - e_{ij}^{Ae} + e_{ij}^{Bp} - e_{ij}^{Ap} = S_{ijkl}^{A}\tau_{kl}^{A} - S_{ijkl}^{B}\tau_{kl}^{B}\,.$$

From these 6 equations three equations for Δe_{11}, Δe_{33} and Δe_{13} can be used for calculation of non-zero components of τ_{ij}^{A}, τ_{ij}^{B}. Using eq. (6) and (1d) we have

$$\Delta e_{ij} = e_{ij}^{Be} + e_{ij}^{Bp} - e_{ij}^{Ae} - e_{ij}^{Ap} \quad \text{for} \quad ij = 11, 33, 13$$

and

$$\Delta e_{ij} = -(S_{ijkl}^{A} + S_{ijkl}^{B})\,\tau_{kl}^{B} \quad \text{for} \quad ij = 11, 33, 13\,.$$

In the matrix notation we can write for the compatibility stresses

$$\begin{pmatrix} \tau_{11} \\ \tau_{33} \\ \tau_{13} \end{pmatrix} = -\operatorname{sgn} x_2 \begin{pmatrix} s_{11}^{+} & s_{13}^{+} & s_{15}^{+} \\ s_{13}^{+} & s_{33}^{+} & s_{35}^{+} \\ s_{15}^{+} & s_{35}^{+} & s_{55}^{+} \end{pmatrix} \cdot \begin{pmatrix} \Delta e_{11} \\ \Delta e_{33} \\ \Delta e_{13} \end{pmatrix}, \tag{7}$$

where s_{ij}^{+} are sums of elastic compliances in the usual two-index notation, $s_{ij}^{+} = s_{ij}^{A} + s_{ij}^{B}$. The indexing of the additional stress τ_{ij} is expressed by the function $\operatorname{sgn} x_2$ ($x_2 < 0$ in the grain A and $x_2 > 0$ in the grain B). Note that the induced elastic strains e_{12}, e_{22}, e_{32} are generally non-zero and can be calculated from Hooke's law (4) using the known compatibility stresses τ_{ij}.

Let us assume the special case when the bicrystal is uniaxially loaded at infinity by a constant tensile or compressive stress Σ. Generally the loading axis does not

lie in the grain boundary plane, makes an angle α with the x_3 axis and the projection of the stress axis to the x_1x_2 plane makes an angle β with the x_1 axis (see fig. 1a). For the stress Σ acting along the loading axis, the stress tensor, Σ_{ij}, in our coordinate system will be

$$
\begin{aligned}
&\Sigma_{11} = \Sigma \sin^2\alpha \cos^2\beta\,, \quad \Sigma_{12} = \Sigma \sin^2\alpha \sin\beta \cos\beta\,,\\
&\Sigma_{22} = \Sigma \sin^2\alpha \sin^2\beta\,, \quad \Sigma_{13} = \Sigma \sin\alpha \cos\alpha \cos\beta\,,\\
&\Sigma_{33} = \Sigma \cos^2\alpha\,, \qquad\quad \Sigma_{23} = \Sigma \sin\alpha \cos\alpha \sin\beta\,.
\end{aligned} \tag{8}
$$

3. PARTICULAR CASES

3.1. Elastically isotropic media

When the two parts of a bicrystal are elastically isotropic and made of the same material, the difference between the elastic strains is equal to zero since the elastic deformation is the same in the two grains. The additional stresses may arise as a result of incompatible plastic deformation or when the bicrystal is made of isotropic materials characterized by different elastic constants. The elastic compliances, s_{ij}, for an isotropic continuum can be expressed by the Young modulus, E, and the Poisson ratio, ν, in the following way

$$
\begin{aligned}
&s_{11} = s_{33} = 1/E\,, \quad s_{13} = -\nu/E\,,\\
&s_{15} = s_{35} = 0\,, \qquad s_{55} = 2(1+\nu)/E\,.
\end{aligned}
$$

3.1.1. Plastic deformation of elastically isotropic bicrystals

Let us consider the case when the two grains of the bicrystal possess the same elastic constants, however, are differently plastically deformed, i.e. the plastic strains determined by equation (5) are different in the crystals A and B. It can happen when the bicrystal is made for example of tungsten, which is almost elastically isotropic, when the crystallographic orientations of the stress axis are different in the two grains, the Schmid factors have different magnitudes and hence the slip is activated on different slip systems or in particular, only in one grain while the other grain is not plastically deformed. According to equation (7) the additional stresses can be written as

$$
\begin{aligned}
\tau_{11} &= -\operatorname{sgn} x_2 (\Delta e^{\mathrm{p}}_{11} + \nu\, \Delta e^{\mathrm{p}}_{33})\, \mu/(1-\nu)\,,\\
\tau_{33} &= -\operatorname{sgn} x_2 (\nu\, \Delta e^{\mathrm{p}}_{11} + \Delta e^{\mathrm{p}}_{33})\, \mu/(1-\nu)\,,\\
\tau_{13} &= -\operatorname{sgn} x_2\, \Delta e^{\mathrm{p}}_{13}\, \mu/2\,,
\end{aligned} \tag{9}
$$

where $\Delta e^{\mathrm{p}}_{ij}$ is the difference between the plastic strains in grains B and A and μ is the shear modulus which is equal to $\frac{1}{2}E/(1+\nu)$. The same result has been obtained using a different method for calculation of additional stresses in [6].

3.1.2. Deformation of bicrystals formed by two different elastically isotropic materials

Now we will consider an interface between two elastically isotropic materials with different elastic constants. This model can be applied to composite materials made of isotropic components. The arising additional stresses can be expressed as a function of differences between strains in grains B and A, Δe_{ij}, if they are deformed separately by the external applied stress and then connected

$$(10) \qquad \begin{pmatrix} \tau_{11} \\ \tau_{33} \end{pmatrix} = -\operatorname{sgn} x_2 Y \begin{pmatrix} E^{\mathrm{A}} + E^{\mathrm{B}} & \nu^{\mathrm{A}}E^{\mathrm{B}} + \nu^{\mathrm{B}}E^{\mathrm{A}} \\ \nu^{\mathrm{A}}E^{\mathrm{B}} + \nu^{\mathrm{B}}E^{\mathrm{A}} & E^{\mathrm{A}} + E^{\mathrm{B}} \end{pmatrix} \begin{pmatrix} \Delta e_{11} \\ \Delta e_{33} \end{pmatrix},$$

$$\tau_{13} = -\operatorname{sgn} x_2 \, \Delta e_{13} \, \mu^{\mathrm{A}}\mu^{\mathrm{B}}/(\mu^{\mathrm{A}} + \mu^{\mathrm{B}}),$$

where the constant Y is given as

$$Y = E^{\mathrm{A}}E^{\mathrm{B}}/\left(\left(E^{\mathrm{B}}(1 + \nu^{\mathrm{A}}) + E^{\mathrm{A}}(1 + \nu^{\mathrm{B}})\right) \cdot \left(E^{\mathrm{B}}(1 - \nu^{\mathrm{A}}) + E^{\mathrm{A}}(1 - \nu^{\mathrm{B}})\right)\right).$$

3.2. Elastically anisotropic media

In this section we will consider bicrystals made of component crystals of cubic symmetry. The elastic material parameters can be given as elastic stiffnesses, c°_{11}, c°_{12}, c°_{44}, or as elastic compliances, s°_{11}, s°_{12}, s°_{44}, in the commonly used two-index notation. The anisotropy factor A is equal to

$$A = 2c^{\circ}_{44}/(c^{\circ}_{11} - c^{\circ}_{12}).$$

The superscript "o" indicates that the elastic constants are expressed in the cubic crystallographic coordinate system. The elastic compliances referred to a general coordinate system are given by s°_{ij} and the transformation matrix of the cubic crystallographic directions, a_{ij},

$$S_{klmn} = s^{\circ}_{12}\delta_{kl}\delta_{mn} + \tfrac{1}{4}s^{\circ}_{44}(\delta_{km}\delta_{ln} + \delta_{kn}\delta_{ln}) + \vartheta \sum_{i=1}^{3} a_{ki}a_{li}a_{mi}a_{ni},$$

where $\vartheta = s^{\circ}_{11} - s^{\circ}_{12} - \frac{1}{2}s^{\circ}_{44}$. The four-index tensor S_{klmn} is expressed in the two-index notation according to the replacements $11 \to 1$, $22 \to 2$, $33 \to 3$, $32 \to 4$, $31 \to 5$, $21 \to 6$ and equations [12]

$$\begin{aligned} S_{klmn} &= s_{ij} \quad \text{for} \quad i, j \leqq 3, \\ 2S_{klmn} &= s_{ij} \quad \text{for} \quad i \text{ or } j > 3, \\ 4S_{klmn} &= s_{ij} \quad \text{for} \quad i, j > 3. \end{aligned}$$

In the following paragraphs we will discuss two classes of bicrystals, namely, the bicrystals containing tilt grain boundaries with the rotation axes ⟨100⟩ and ⟨110⟩.

3.2.1. Elastic deformation of ⟨100⟩ tilt bicrystals loaded along the axis parallel to the boundary plane

When a bicrystal is deformed elastically the difference in strains between B and A grains, Δe_{ij}, is caused entirely by the elastic anisotropy of the component crystals and it is a function of the applied stress only. The dependence of the additional stresses on the magnitude of the applied stress, Σ, and on its direction given by the angle α between the loading axis and the $[\bar{1}00]$ rotation axis can be written in a simple form

$$\begin{pmatrix} \tau_{11} \\ \tau_{33} \\ \tau_{13} \end{pmatrix} = -\operatorname{sgn} x_2 \Sigma \sin^2 \alpha Q \begin{pmatrix} s_{11}^{\circ} \\ -s_{12}^{\circ} \\ 0 \end{pmatrix}, \tag{11}$$

where Q depends on the crystallographic orientations of the A and B crystals in the common coordinate system of the bicrystal

$$Q = \vartheta(\sin^2 2\varphi^{A} - \sin^2 2\varphi^{B})/[s_{11}^{\circ}(4s_{11}^{\circ} - \vartheta(\sin^2 2\varphi^{A} + \sin^2 2\varphi^{B}) - 4s_{12}^{\circ}],$$
$$\vartheta = s_{11}^{\circ} - s_{12}^{\circ} - \tfrac{1}{2}s_{44}^{\circ}.$$

Only bicrystals stressed along the axis lying in the boundary plane are considered in this paragraph. Then the angle β in equation (8) is equal to zero. The crystallographic orientation of the grains is determined by the angles φ^{A}, φ^{B} between the grain boundary normal, x_2, and the [010] axes in the grains A and B, respectively. The [100] crystallographic direction parallel to the rotation axis is identical in the two grains.

For example, for the misorientation $\Delta\varphi = 36{\cdot}88°$ which corresponds to the reciprocal density of coincidence sites equal to 5, the angle φ^{B} depends on the angle φ^{A} which determines the crystallographic orientation of the boundary normal in the grain A, $\varphi^{B} = \varphi^{A} + 36{\cdot}88°$. If $\varphi^{A} = -18{\cdot}44°$ or $26{\cdot}52°$ we get symmetrical grain boundaries on the {013} or {012} planes, respectively, and the additional stresses are equal to zero. When the boundary normal bisects the angle between the normals to the respective {013} and {012} planes, i.e. when $\varphi^{A} = 4{\cdot}04°$, then all the nonzero components of the additional stress tensor are close to the maximum values. This special orientation of the boundary plane, $(0\,1\,14)^{A}/(0\,20\,23)^{B}$ was chosen for the experimental investigation of the effects of additional compatibility stresses [13].

The dependence of the additional stresses on the orientation of the grain boundary normal for a fixed misorientation of 36·88° and for elastic constants of silicon-iron alloy, Fe–3 wt. % Si, ($s_{11}^{\circ} = 8{\cdot}75$, $s_{12}^{\circ} = -3{\cdot}356$, $s_{44}^{\circ} = 8{\cdot}23 \times 10^{-12}\,\mathrm{Pa}^{-1}$ and $A = 2{\cdot}94$) has already been discussed in our earlier paper [14]. Here we will focus on those grain boundaries where the compatibility effects are strongest. In fig. 2 the angle φ^{A}, for which the maximum values of τ_{11} and τ_{33} are reached, is plotted as a function of the misorientation angle, $\Delta\varphi = \varphi^{B} - \varphi^{A}$, for two magnitudes of the anisotropy factor corresponding to Fe–3 wt. % Si ($A = 2{\cdot}94$) and β-brass ($A = 8{\cdot}91$). Full line denotes the limit $A = 0$. The dependences of compatibility stresses on the orientation of the grain boundary normal for a fixed misorientation are more

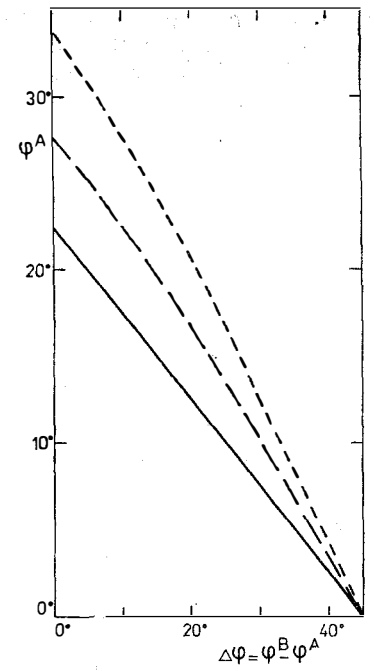

Fig. 2. The orientation of the grain boundary normal (given by φ^{A}), for which the additional compatibility stresses have a maximum, as a function of misorientation $\Delta\varphi$. Full line corresponds to the angle φ^{A} which bisects the dihedral angle of two symmetrical grain boundary planes. Long and short dashed lines were calculated for Fe–3 wt. % Si ($A = 2{\cdot}94$) and β-brass ($A = 8{\cdot}91$), respectively.

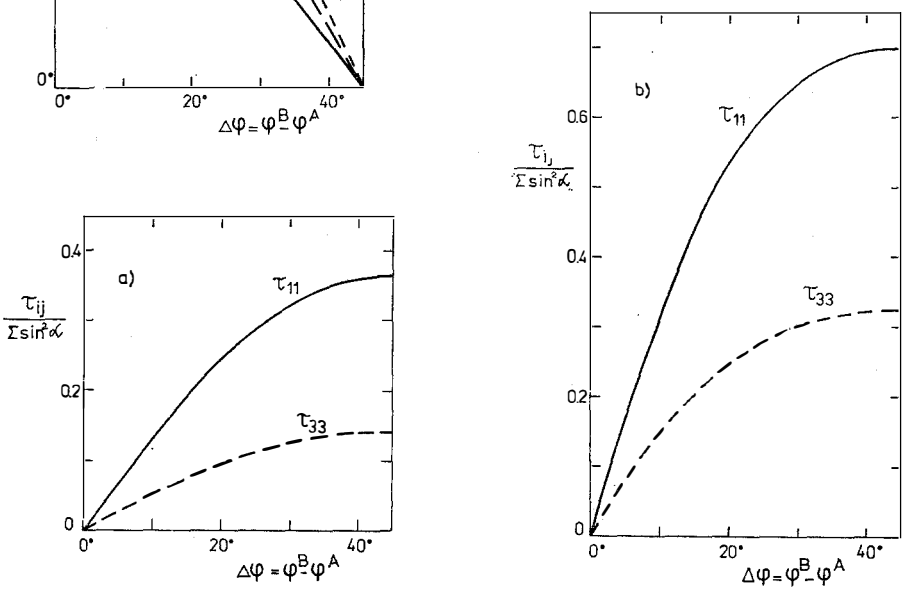

Fig. 3. Maximum values of the additional compatibility stresses as a function of the misorientation angle $\Delta\varphi$. Full and dashed lines denote the τ_{11} and τ_{33} tensor components. Figure a) and b) were calculated for the elastic constants of Fe–3 wt. % Si and β-brass, respectively.

asymmetric for increasing anisotropy factor. Only for relatively small anisotropy factors and for large misorientation angles, the orientation of the boundary normal for the maximum compatibility stresses bisects the angle between boundary normals of symmetrical grain boundaries with zero compatibility stresses. Maximum values of compatibility stress tensor components τ_{11} and τ_{33} are depicted in fig. 3. Remaining tensor components are equal to zero in the chosen coordinate system. The elastic

compliances used in the calculations for β-brass (Cu–46 wt. % Zn) are $s^{\circ}_{11} = 40{\cdot}95$, $s^{\circ}_{12} = -18{\cdot}93$, $s^{\circ}_{44} = 13{\cdot}44 \times 10^{-12}\ \mathrm{Pa}^{-1}$. Comparing fig. 3a and fig. 3b a strong dependence of compatibility stresses on the magnitude of the anisotropy factor is clearly demonstrated.

3.2.2. Elastic deformation of ⟨100⟩ tilt bicrystals loaded along the axis inclined to the boundary plane

In all other particular cases in this paper we consider the deformation of bicrystals along the loading axis parallel to the grain boundary plane ($\beta = 0$). Only here we will deal with the case when the angle β in equations (8) (see also fig. 10) is equal to 90°. Then the angle α between the loading axis with the $[\bar{1}00]$ rotation axis describes the inclination of the loading axis which varies from the rotation axis to the grain boundary normal, x_2. In the expression for the additional compatibility stresses (7), the s^{+}_{ij} quantities ($i, j = 1, 3, 5$) depend only on the misorientation of the grains and on the orientation of the grain boundary plane while Δe_{ij} also include a dependence on the orientation of the loading axis. The non-zero components of the Σ_{ij} tensor (see equations (4)) for $\beta = 90°$ are Σ_{22}, Σ_{33} and Σ_{23}. Now the only non-zero component of Δe^{e}_{ij} is Δe^{e}_{11} which is equal to

$$\Delta e^{e}_{11} = (s^{B}_{12} - s^{A}_{12})\,\Sigma_{22}\,,$$

where $s_{12} = s^{\circ}_{12} + \frac{1}{2}\vartheta \sin^2 2\varphi$, $\vartheta = s^{\circ}_{11} - s^{\circ}_{12} - \frac{1}{2}s^{\circ}_{44}$ for the x_3 axis parallel to the $[\bar{1}00]$ rotation axis. Then inserting to equation (7) we get

$$\begin{pmatrix} \tau_{11} \\ \tau_{33} \\ \tau_{13} \end{pmatrix} = -\operatorname{sgn} x_2 \Sigma \sin^2 \alpha Q \begin{pmatrix} s^{\circ}_{11} \\ -s^{\circ}_{12} \\ 0 \end{pmatrix}, \tag{12}$$

where Q is again equal to

$$Q = \vartheta(\sin^2 2\varphi^{A} - \sin^2 2\varphi^{B})/[s^{\circ}_{11}(4s_{11} - \vartheta(\sin^2 2\varphi^{A} + \sin^2 2\varphi^{B}) - 4s^{\circ}_{12}]\,.$$

Notice that this expression is almost identical with (11), the only difference in the dependence of the additional stresses on the angle α is the changed sign of the stresses in (12) which follows from the transformation of s_{12} as a function of crystal rotation by φ.

3.2.3. Plastic deformation of ⟨100⟩ tilt bicrystals

In this paragraph we will study compatibility stresses arising when one grain is deformed plastically and the other grain is strained elastically only. We will consider an asymmetrical bicrystal with the misorientation of 37° and the boundary plane on $(0\ 1\ 14)^{A}/(0\ 20\ 23)^{B}$. The homogeneous shear deformation is caused by the operation of a single slip in the [111] direction on the plane with maximum resolved shear stress in the A grain. The slip plane orientation changes between $[\bar{2}11]$ and $[\bar{1}\bar{1}2]$

with the $(\bar{1}01)$ reference plane for α increasing from 0° to 46° and between $[\bar{1}\bar{1}2]$ and $[1\bar{2}1]$ with the $(0\bar{1}1)$ reference plane for α rising from 46° to 86°. The magnitude of shear deformation, γ, was chosen to be 0·1.

The compatibility stresses, τ_{ij}, can be calculated again from equation (7) where the elastic compliances, s_{ij}, have a simple form $s_{11} = s_{11}^{\circ} - \frac{1}{2}\vartheta \sin^2 2\varphi$, $s_{13} = s_{12}^{\circ}$, $s_{33} = s_{11}^{\circ}$, $s_{55} = s_{44}^{\circ}$ and $s_{15} = s_{35} = 0$ in the used coordinate system (the x_3 axis is parallel to the $[\bar{1}00]$ rotation axis, the x_2 axis is perpendicular to the grain boundary plane and hence the x_1 axis lies also in the boundary as shown in fig. 1a). When plastic deformation is taken into account, the elastic strains must be considered for the flow stress under which the A grain with higher Schmid factor is plastically deformed. The strain differences are given by equations (4, 5).

For a comparison with experiments it is important to know shear stresses acting on various slip systems. We will not discuss the dependence of compatibility stresses on the loading direction here, instead we will assess the effect of plastic deformation on shear stresses resolved to four possible slip systems as it is done in the next paragraph.

3.2.4. Modification of resolved shear stresses by the additional compatibility stresses

Redistribution of stresses in a bicrystal due to the requirements on the compatibility of elastic and plastic strains can lead to the initiation of slip systems which would not operate in separated grains or to the suppression of some of the active slip systems. To explain such effects it is essential to determine the resolved shear stresses, RSS, for four possible slip systems given by the $\langle 111 \rangle$ slip directions in b.c.c. metals. The orientation of the slip plane in b.c.c. metals has been discussed in detail in a recent review [15]. It was shown that at room temperature, the slip plane is close to the plane with maximum RSS. A deviation of the actual slip plane from the maximum RSS plane increases with decreasing temperature. In this paper a complex character of slip will not be considered, we will assume that the slip plane is the plane with maximum RSS for each respective slip direction.

First we will estimate the magnitude of elastic compatibility stresses in the coordinate systems attached to the loading axis (now parallel to the x_3 axis). The grain boundary normal is still parallel to the x_2 axis. Again we will consider the asymmetrical bicrystal with the $\langle 100 \rangle$ rotation axis, the $(0\,1\,14)^{A}/(0\,20\,23)^{B}$ boundary plane and the loading axis lying in the boundary. The dependences of non-zero components of the transformed compatibility stress tensor T_{ij} as a function of the angle α are depicted in fig. 4 for the elastic constants of Fe–3 wt.% Si and β-brass. The compatibility stresses due to the anisotropic elastic deformation are positive in the B grain and negative in the A grain. For $\alpha < 45°$, the component T_{11} (perpendicular to the loading axis) is higher than T_{33}. On the other hand, for $\alpha > 45°$, T_{33} which is parallel to the loading axis is significantly larger. The orientation of respective slip planes for all four $\langle 111 \rangle$ slip systems in the calculations of the RSS was determined in the following way. The normal to the slip plane, $\boldsymbol{n}$, is expressed

as a linear combination of two chosen vectors, $\boldsymbol{n}_1$ and $\boldsymbol{n}_2$, perpendicular to the slip direction, $\boldsymbol{b}$, which is parallel to the respective Burgers vector

$$\boldsymbol{n} = \boldsymbol{n}_1 + \lambda \boldsymbol{n}_2 , \quad \boldsymbol{n}_1 \boldsymbol{b} = \boldsymbol{n}_2 \boldsymbol{b} = 0 .$$

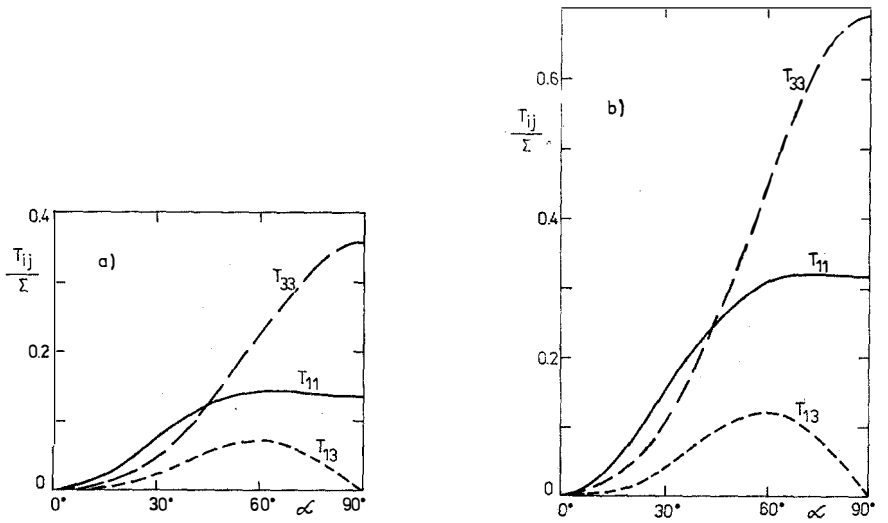

Fig. 4. Components of the compatibility stress tensor in the coordinate system where the x_3 axis is parallel to the loading axis (x_2 is still perpendicular to the boundary) as a function of the angle α between the loading and $\langle 100 \rangle$ rotation axes. The asymmetrical $\langle 100 \rangle$ tilt bicrystal $(0\,1\,14)^{A}/(0\,20\,23)^{B}$ is deformed elastically only. Figure a and b are for Fe–3 wt. % Si and β-brass, respectively.

For example, if the $\boldsymbol{n}_1$ and $\boldsymbol{n}_2$ vectors are parallel to $[0\bar{1}1]$ and $[\bar{1}01]$, respectively, the orientation of the slip plane normal in the range from $[1\bar{2}1]$ to $[\bar{1}\bar{1}2]$ (for $\boldsymbol{b}$ parallel to $[111]$) is described by λ from the interval $\langle -0{\cdot}5, 1 \rangle$. The resolved shear stress, σ, for a slip system defined by $\boldsymbol{b}$ and $\boldsymbol{n}$ can be written as

$$\sigma = \sigma_{ij} b_i n_j ,$$

where $\boldsymbol{b}$ and $\boldsymbol{n}$ are normalized unit vectors. The magnitude of parameter λ is obtained from the condition that RSS attains a maximum value

$$\mathrm{d}\sigma/\mathrm{d}\lambda = 0 ,$$

which thus determines the orientation of the slip plane, namely, the plane with maximum RSS for a considered slip direction.

The dependences of the RSS, σ, on the orientation of the loading axis, α, ($\beta = 0$) are shown in fig. 5 for the applied stress, i.e. without the additional compatibility stresses, as full lines. The short dashed lines represent the total RSS which include the additional stress due to the elastic anisotropy. Finally, the long dashed lines were calculated for the shear plastic deformation $\gamma = 0{\cdot}1$ in the A grain on the slip system

[111] at the applied stress of 350 MPa which corresponds to the flow stress. In this case, the resulting stress is a sum of the applied stress and the compatibility stresses due to the anisotropic elastic deformation and due to the plastic deformation which occurs in the A grain only. Again the asymmetrical bicrystal $\langle 100\rangle (0\ 1\ 14)^{A}/(0\ 20\ 23)^{B}$ of Fe–3 wt. % Si was considered. It is seen in fig. 5 that the shear deformation in the [111] direction in the A grain increases essentially the RSS in the A grain, in particular for the [111] and [11$\bar{1}$] significant slip systems while the effect of elastic compatibility decreases the stress level of the applied stress. In the B grain, this shear deformation

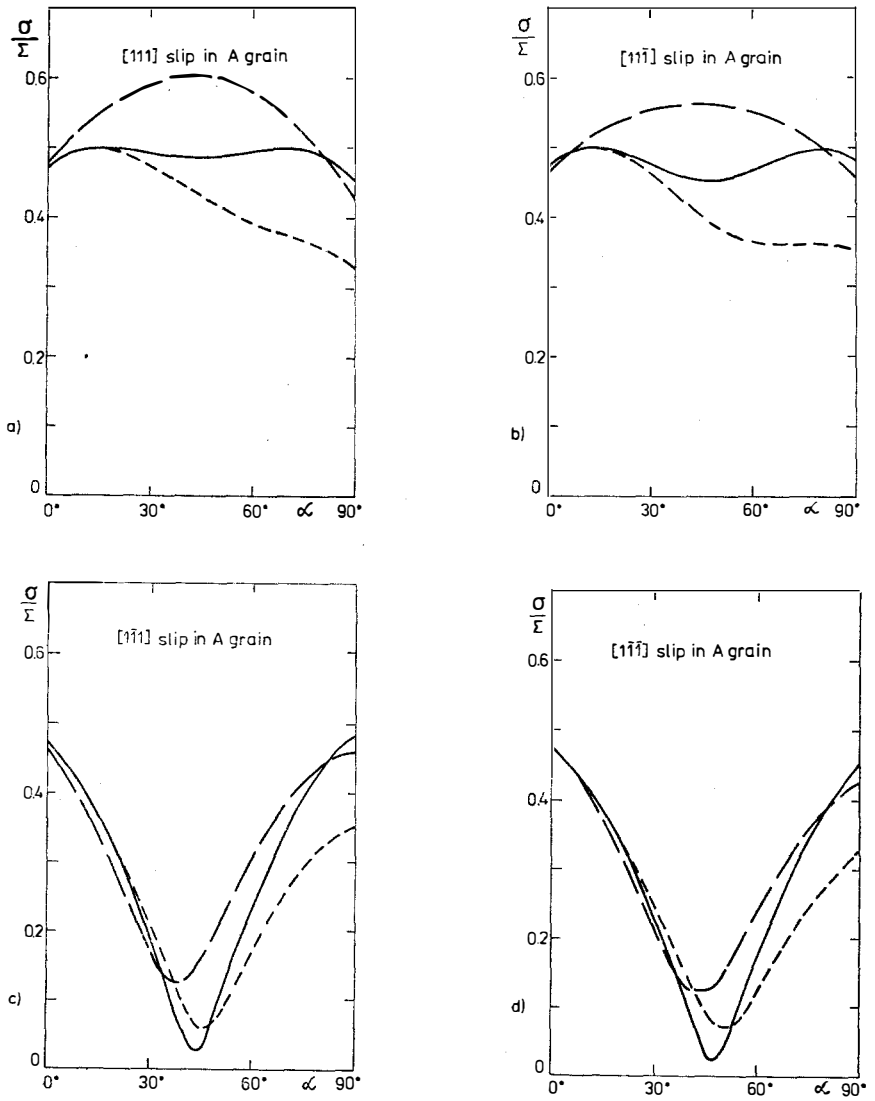

Fig. 5. *(continued)*

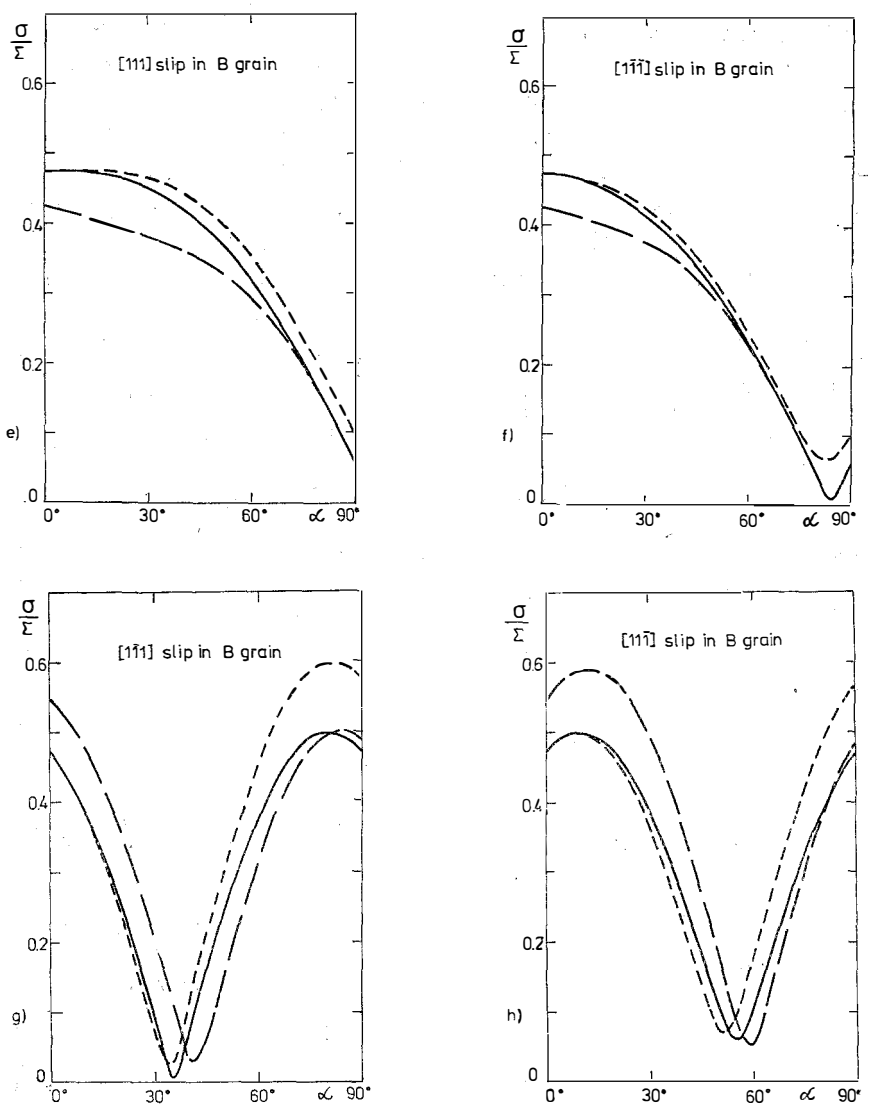

Fig. 5. Resolved shear elastic and plastic compatibility stresses for all four possible slip systems as functions of the orientation of the loading axis with respect to the ⟨100⟩ rotation axis. Full, short-dashed and long-dashed lines were calculated for the external applied stress, for the sum of the applied and elastic compatibility stresses and for the total stress including both elastic and plastic compatibility stresses, respectively. The A or B grain and the respective slip systems are indicated in each figure. The stresses are normalized by the magnitude of the external applied stress, Σ.

decreases the stress level for the [111] and [1$\bar{1}\bar{1}$] slip systems, where the elastic compatibility leads to a slight stress increase, and also changes the stress level in the opposite direction than the elastic compatibility for the [1$\bar{1}$1] and [11$\bar{1}$] slip systems.

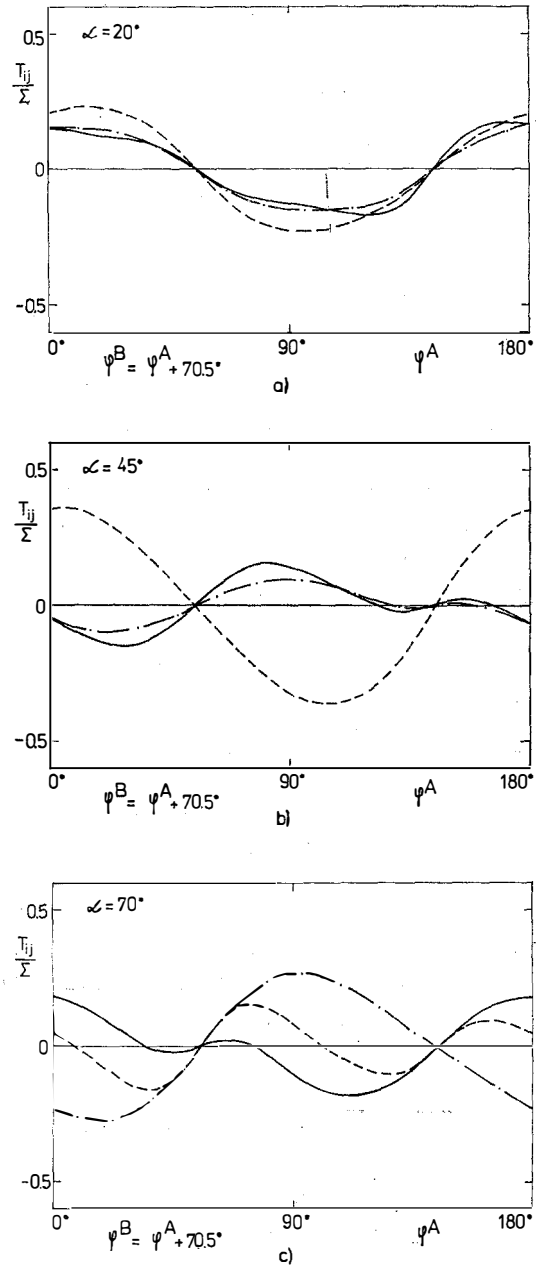

Fig. 6. Components of the compatibility stress tensor for $\langle 110 \rangle$ tilt bicrystals with the misorientation of 70·53°. The angle φ^A determines the orientation of the grain boundary normal, α is the angle between loading and rotation axes. Full, dashed and dot-dashed lines denote T_{11}, T_{33} and T_{13} stress components, respectively.

The effect of the plastic deformation is given by the difference between long-dashed and short-dashed lines in fig. 5. It should be emphasized that the additional stresses due to compatibility of anisotropic elastic deformation have a magnitude comparable with the additional stresses due to compatibility of shear plastic deformation of the order of $\gamma \approx 10\%$ which took place only in one grain. Hence the effect of elastic compatibility is negligible only for very large plastic strains.

3.2.5. Elastic deformation of ⟨110⟩ tilt bicrystals loaded along the axis parallel to the boundary plane

When the rotation axis is parallel to ⟨110⟩, i.e. has a lower symmetry, it is not possible in the expression for additional compatibility stresses (τ_{ij}, $ij = 11, 33, 13$) to separate the dependence on the boundary plane orientation and on the loading axis orientation as it was done in equation (11). In fig. 6 the non-zero components of the compatibility stress tensor are depicted for three values of the angle α (which makes the loading axis with the rotation axis) as functions of the orientation of the boundary plane normal for a fixed misorientation of $\varphi^B - \varphi^A = 70{\cdot}53°$ corresponding to the reciprocal density of coincidence sites equal to 3. The stress components were calculated in the coordinate system where x_3 is parallel to the loading axis and x_2 is perpendicular to the grain boundary plane according to the following transformation of τ_{ij} given by (7)

$$
\begin{aligned}
T_{11} &= \tau_{11}\cos^2\alpha + \tau_{33}\sin^2\alpha - \tau_{13}\sin 2\alpha\,, \\
T_{33} &= \tau_{11}\sin^2\alpha + \tau_{33}\cos^2\alpha + \tau_{13}\sin 2\alpha\,, \\
T_{13} &= (\tau_{11} - \tau_{33})\sin 2\alpha/2 + \tau_{13}\cos 2\alpha\,.
\end{aligned} \tag{13}
$$

Notice that the compatibility stresses are equal to zero for symmetrical grain boundaries when $\varphi^A = 54{\cdot}74°$ and $144{\cdot}74°$ which corresponds to the boundary planes on {111} and {112}. φ^A denotes again the angle between the boundary normal and the ⟨001⟩ direction which is perpendicular to the ⟨110⟩ rotation axis. The elastic constants of Fe–3 wt. % Si were employed. In fig. 7 the variation of the compatibility

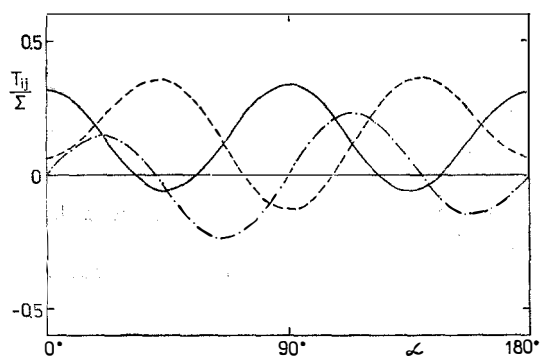

Fig. 7. Compatibility stresses for the $(001)^A/(2\bar{2}1)^B$ asymmetrical bicrystal as functions of the angle α between the loading and rotation axes. Different lines denote the same quantities as in fig. 6.

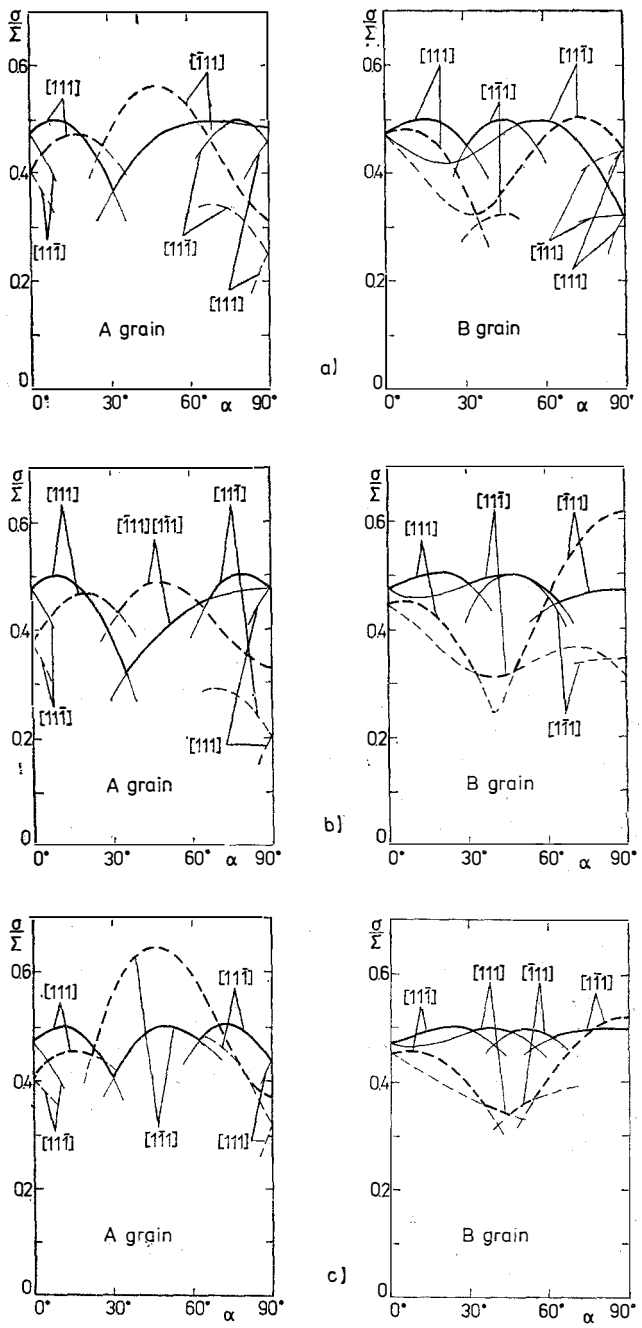

Fig. 8. Maximum resolved elastic compatibility shear stresses for asymmetrical bicrystals with the ⟨110⟩ rotation axis. a), b) and c) show the dependences for the inclinations of the grain boundary plane to $(001)^A$ of 75°, 90° and 120°, respectively. The stresses are normalized by the magnitude of the applied stress. Full and dashed lines correspond to the applied and total stress tensors.

stresses is shown as a function of α for a chosen asymmetrical bicrystal $(001)^A/(2\bar{2}1)^B$ still with the same misorientation of 70·53°. It is seen that all three non-zero stress components reach maximum magnitudes of the order 0·3 of the applied stress, however, the maxima for different components are reached at different values of α for fixed φ^A and φ^B (fig. 7) or at different values of φ^A for fixed α and $\Delta\varphi = \varphi^B - \varphi^A$ (fig. 6). In both fig. 6 and 7 only the stress components in the A grain are depicted since in the B grain they have the same magnitude but the opposite sign according to (8).

It has been stressed in section 3.2.4 that the shear stresses resolved for various slip systems are necessary for the interpretation of experimental results. Let us consider three asymmetrical bicrystals with the inclination to the $(001)^A$ plane 75°, 90° and 120°, i.e. with the grain boundary planes lying approximately on $(5\bar{5}2)^A/(\bar{1}12)^B$, $(\bar{1}10)^A/(\bar{1}14)^B$ and $(\bar{5}54)^A/(\bar{1}18)^B$ respectively. In all three cases the misorientation angle with respect to the [110] rotation axis is 70·53°. Again the shear stresses were calculated for each shear direction of the $\langle 111 \rangle$ type on planes with the maximum resolved shear stress. In fig. 8 RSS normalized by the applied stress Σ are plotted as a function of the orientation of the loading axis given by the angle α. Only values for slip systems with the maximum stress level are depicted. The full lines correspond to the applied stress tensor and the dashed lines correspond to the total stress tensor including the additional stress due to compatibility of elastic deformation. The computation was performed again for the elastic constants of Fe–3 wt. % Si.

Plastic behaviour of an asymmetrical bicrystal with a chosen loading axis can be predicted from fig. 8 in the following way. First compare the applied stress level in the A and B grains. If the maximum RSS in both grains are of about the same magnitude, the plastic deformation on appropriate slip systems can be expected in the interiors of both grains far from the boundary. When maximum RSS is higher in one grain, only the interior of this grain will be plastically deformed in the early deformation stages. Now let us concentrate on the total stress level including the elastic compatibility stress. If the total stress level (dashed line) is higher than the applied stress level (full line), the slip will be more intense near the boundary and will initiate there. On the other hand if the total stress level is lower than the applied stress level, the slip activity will decrease towards the boundary. It may also happen that the applied stress level in one grain is low but the total stress level in this grain is sufficiently high. Then the plastic deformation will be localized only in the boundary region. Of course, since the compatibility of plastic strains has not been taken into account in fig. 8, it is applicable only to early deformation stages.

4. DISCUSSION

The model described in this paper enables us to analyse the compatibility stresses in dependence on various parameters which characterize the type of grain boundary and the loading direction. However, the results of the model are applicable, strictly

speaking, only to the middle part of the thin region adjacent to the interface, far from its edges. The distribution of stresses in bicrystals with finite dimensions in the boundary plane has been studied in a few special cases in literature. Chou and Hirth [16] considered two elastic isotropic media differing in the magnitude of shear modulus. The shape of each grain was a semiinfinite plate and the area of the interface separating the grains had a finite width equal to the thickness of the plates. For the uniform applied compressive (normal to the plate) and shear stresses (with both shear plane normal and shear direction lying in the interphase boundary plane), the compatibility stresses decrease exponentially with the distance from the interface. At a distance from the interface greater than the plate thickness, the compatibility stresses approach zero.

The stress distribution in finite bicrystals loaded in the direction parallel to the interface was calculated using the finite element method in [17]. The stresses were determined for two types of bicrystals and their dependence on the grain shape was investigated. The grain shape was described by the bicrystal dimensions in the direction lying in the boundary perpendicularly to the loading axis (thickness) and in the direction normal to the boundary (width). For the thickness smaller than the width the variations of the stress tensor were localized near to the grain boundary similarly as in [16], while for the thickness greater than the width the stress variations spread practically to the whole grains. The peak values of the compatibility stresses at the grain boundary were found to be proportional to the anisotropy factor of considered cubic crystals. Maximum resolved shear stresses were always reached at the intersection of the grain boundary with the free surface of the bicrystal.

It is obvious that the effect of the free surfaces on the stress distribution in finite bicrystals is fairly complicated in particular for the grains with rectangular cross-section having the longer side attached to the other grain. Then all particular cases have to be treated separately and it is necessary to consider in addition to the crystallographic parameters (rotation of the grains, orientations of the boundary normal and of the loading axis) also the ratios of sample dimensions. The model used in the present paper provides an evaluation of compatibility stresses which can be easily applied to various types of bicrystals. Although it does not give the detailed stress distribution it is useful for a systematic investigation of the compatibility stresses near the interface as functions of relatively large number of crystallographic parameters.

Compatibility stresses were calculated by means of finite element method also in [18]. However, only a two-dimensional model was used and thus the crystal anisotropy could not be fully taken into account. In [19] the finite element method was applied to a polycrystalline sample. The two-dimensional method was adapted for a three-dimensional problem and the anisotropic elastic constants of cubic α-brass were employed. The results of the model were compared with the observation of slip onset in the sample with the grain size of 2·5 mm. On the basis of a detailed analysis it was concluded that the elastic compatibility stresses play an important

role in the yield process and may exercise influence for strains of at least several percent. This conclusion is in agreement with the quantitative evaluation of the relative influence of plastic deformation and elastic compatibility stresses as discussed in sec. 3.2.4 in the present paper.

Besides the compatibility stresses, grain boundaries have a pronounced influence also on the distribution of dislocations which are sources of internal stresses. In dependence on dislocation properties and mutual orientation of possible slip systems, the lattice dislocations can be stopped on the slip plane by the grain boundary, may cross-slip in front of the boundary, can be transmitted into the other grain forming residual grain boundary dislocations or may spread into the grain boundary. Stress discontinuities and the structure imperfections at the grain boundary may activate dislocation sources which significantly affect plastic deformation. Though the effect of grain boundaries on mechanical properties is rather complex, the macroscopic distribution of stresses is an important factor that cannot be neglected. The results of our model were compared with the observation of slip activity in an asymmetrical bicrystal loaded along different directions parallel to the boundary plane [13]. In spite of the fact that all details of slip pattern, in particular activation of extra slip systems related to the dislocation transfer from one grain to another one, cannot be explained using an elastic continuum model, the overall slip activity is controlled by the sum of applied and compatibility stresses.

References

[1] Livingston J. D., Chalmers B.: Acta Metall. *5* (1957) 322.
[2] Hauser J. J., Chalmers B.: Acta Metall. *9* (1961) 802.
[3] Hook R. E., Hirth J. P.: Acta Metall. *15* (1967) 535.
[4] Hook R. E., Hirth J. P.: Acta Metall. *15* (1967) 1099.
[5] Hirth J. P.: Metall. Trans. *3* (1972) 3047.
[6] Rey C., Zaoui A.: Acta Metall. *28* (1980) 687.
[7] Rey C., Zaoui A.: Acta Metall. *30* (1982) 523.
[8] Berveiller M.: Thesis. Université Paris-Nord, Villetaneuse, 1978.
[9] Berveiller M.: Science et techniques de l'armement *54* (1980) 521.
[10] Bogy D. B.: J. Appl. Mech. *72* (1975) 93.
[11] Rieder G.: Abhandlungen der Braunschweigischen Wissenschaftlichen Gesellschaft, Band *XI* (1959), 20.
[12] Steeds J. W.: Anisotropic Elasticity Theory of Dislocations. Clarendon Press, Oxford, 1973.
[13] Šittner P., Paidar V.: Acta Metall. *37* (1989) — to be published.
[14] Gemperlová J., Paidar V.: Czech. J. Phys. B *35* (1985) 351.
[15] Christian J. W.: Metall. Trans. A *14* (1983) 1237.
[16] Chou T. W., Hirth J. P.: J. Composite Materials *4* (1970) 102.
[17] Kitagawa K., Asada H., Monzen R., Kichuki M.: *in* Proc. JIMIS-4, Suppl. Trans. Japan Inst. Metals *27* (1986) 827.
[18] Meyers M. A., Ashworth E.: Philos. Mag. A *46* (1982) 737.
[19] Hashimoto K., Margolin H.: Acta Metall. *31* (1983), 773.